

# Measurement-based wireless network planning, monitoring, and reconfiguration solution for robust radio communications in indoor factories

ISSN 1751-8822

Received on 18th September 2015

Revised on 10th December 2015

Accepted on 18th December 2015

doi: 10.1049/iet-smt.2015.0213

www.ietdl.org

Xu Gong , Jens Trogh, Quentin Braet, Emmeric Tanghe, Prashant Singh, David Plets, Jeroen Hoebeke, Dirk Deschrijver, Tom Dhaene, Luc Martens, Wout Joseph

Department of Information Technology, Ghent University/iMinds, Gaston Crommenlaan 8 bus 201, 9050 Ghent, Belgium

E-mail: xu.gong@intec.ugent.be

**Abstract:** Nowadays, the harsh industrial environment remains one of the vital challenges for an effective deployment of wireless technologies in factories to promote the industrial upgrade. In this study, a complete solution is proposed for robust radio communications in indoor factories. Herein, measurement setups are integrated with industrial mobile facilities, e.g. an automated guided vehicle and a mobile robot. Calibration is advised for accurately revealing an industrial radio environment. A hybrid sequential design strategy is used to enhance the efficiency of the measurement campaign. This further leads to a surrogate modelling based radio environment map, which facilitates a holistic view and evaluation of the radio quality of service over the target shop floor. In addition, an over-dimensioning heuristic is proposed to guarantee that every target location can be wirelessly covered by at least two access points (APs). Moreover, the smart switch mechanism dynamically powers on/off the over-dimensioned APs, so as to ensure full coverage even at the presence of physical disturbance. The investigation on two real factories and the coverage prediction tool WHIPP further demonstrates the solution's effectiveness. Eventually, a rich outlook is drawn for the roadmap towards an artificially intelligent system for robust industrial wireless communications.

## 1 Introduction

The industry is currently undergoing an emerging evolution closely associated with communication technologies. In the German Industry 4.0 initiative [1], field devices, machines, plants, and factories are envisioned to be connected to a network by means of communication infrastructures. This will further allow storing in the cloud all the documents and knowledge about the physical objects [e.g. three-dimensional (3D) model, topology, process data, etc.]. In North America, analogous ideas have been brought up under the name Industrial Internet [2]. Its target applications are even not limited to industrial production, and include, e.g. smart electrical grids.

Overall, wireless technologies gain dominant popularity over cabled technologies in the various industrial upgrades. In smart factory [3], ubiquitous industrial modular structures are interconnected by various wireless technologies, e.g. WiFi, ZigBee, Bluetooth, 6LoWPAN, cellular networks, WirelessHART, ISA100, and VHF/UHF radios. This enables flexible production processes that will adaptively deal with rapidly changing and personalised customer demands. According to Cisco and Rockwell Automation, the advantages wireless networks can bring to industry include [4]: (i) lower installation costs due to cabling and hardware reduction, (ii) lower operational costs by eliminating cable failures, (iii) ability to connect hard-to-reach and remote areas, and (iv) gains in productivity due to equipment and personnel mobility.

The common wireless industrial applications are summarised in Table 1, with the requirements on important quality of service (QoS) metrics, e.g. latency, packet loss rate, jitter, and availability. They may be run at a range of end-entities, e.g. computer hosts, robots, sensor-mounted autonomous mobile units (e.g. automated guided vehicle or AGV), data-support systems (e.g. servers storing inventory details), and roaming workers with personal digital assistants.

However, radio wave propagation in factories is generally vulnerable, due to the harshness of industrial indoor environments which cause short-term or long-term shadow fading. According to [6], the steel, metals, and rotating machinery often cause the

received signal strength (RSS) to drop as much as 30–40 dB under a short time period. Vehicles, such as trucks and forklifts parking in front of wireless nodes, may eliminate the communication completely. The harshness relevant to the shadow fading can be further illustrated as machinery, containers, racks, and reorganised production lines. As a result, wireless users on the shop floor may often experience a lack of coverage and intermittent connectivity.

Consequently, a solution is proposed in this paper for robust radio communications in indoor factories. This solution is implemented in a unified system, which conducts measurement control, robot mobility control, measurement path optimisation, data visualisation, and solution simulation in a centralised manner. Its contributions are fourfold. (i) Automatic measurements facilitate real-time collection of radio QoS metric(s) from the perspective of clients. A sequential design algorithm proposes efficient measurement paths to the robots. (ii) The surrogate model based radio environment map (REM) enables holistic radio QoS monitoring, and thus an easy identification of coverage holes on the target shop floor. (iii) Over-dimensioning facilitates a redundant wireless coverage, and physically offers highly flexible network reconfigurability against shadow fading. (iv) Extensive industrial empirical measurements and simulation demonstrate this solution's effectiveness for maintaining the robustness of radio communications under the harshness of industrial environments.

Section 2 reviews the recent relevant work and limits the scope of this paper. Section 3 introduces the proposed composite solution. Sections 4 and 5 present the empirical studies and simulation of this solution, respectively. Section 6 draws the conclusion and gives the outlook.

## 2 Literature review and scope

In recent years, there have been rising research interests in the wireless robustness in industrial environments. Herein, large-scale fading in manufacturing factory indoor environments is focused on.

**Table 1** Industrial wireless application and performance requirement

Industrial wireless application	Reference PHY throughput	Sensitivity <sup>a</sup> , dBm	Latency, ms	Packet loss rate	Sensitivity to jitter	Expectation for high or 'always-on' availability
supervisory control	256 kbps	-88	<100	<10 <sup>-9</sup>	yes	yes
distributed I/O <sup>b</sup> control	512 kbps	-88	≈100	<10 <sup>-9</sup>	yes	yes
peer-to-peer control	1 Mbps	-88	<100	<10 <sup>-9</sup>	yes	yes
mobile HMI <sup>b</sup>	1 Mbps	-88	>100	<10 <sup>-4</sup>	no	yes
long haul SCADA <sup>b</sup>	256 kbps	-88	>100	<10 <sup>-4</sup>	yes	yes
asset tracking and RFID <sup>b</sup>	128 kbps	-88	>100	<10 <sup>-4</sup>	no	yes
condition-based monitoring	128 kbps	-88	>100	<10 <sup>-4</sup>	yes	yes
remote video monitoring	24 Mbps	-79	>100	<10 <sup>-4</sup>	yes	yes

<sup>a</sup>The mapping from PHY throughput to sensitivity is based on the reference conversion for a 802.11g chipset at 2.4 GHz [5]

<sup>b</sup>I/O: input/output, HMI: human-machine interface, SCADA: supervisory control and data acquisition, RFID: radio-frequency identification

### 2.1 Characterisation and planning for robustness

In [7], the characterisation of large-scale fading at 3.5 GHz in an office demonstrates the impact of obstacle losses on the reliable estimation of shadow depth. After extensive measurements in a typical living room, large-scale radio channel characteristics are obtained in [8], which include path loss (PL) exponent, standard deviation of shadow fading, and so on. The radio channels in suburban environments were characterised in terms of large-scale fading [9]. However, little characterisation of wireless propagation has been performed in industry. In [10], extensive measurements of RSS at 900, 2400, and 5200 MHz were performed in two wood processing facilities and two metal processing facilities. The investigated factory buildings exhibited similar physical properties: concrete floor, metal ceilings supported by steel truss work, walls made of thick precast concrete, and metal machinery. Based on these measurements, the large-scale fading of industrial radio channels is effectively characterised by a one-slope PL model.

Once the wireless propagation models are characterised, they can be used in wireless planning [11] for a proper link budget calculation which is adapted to the target industrial environment. However, most of the wireless planning solutions are static. They have no association with wireless management, which can dynamically maintain the wireless QoS at the network usage stage. During the planning process, possible major problems are anticipated. The robustness of a network is conventionally increased by accounting for a shadowing margin, a fading margin, or an interference margin. Consequently, this static planning only shows a partial capability to efficiently protect against coverage gaps caused by various shadowing effects in harsh industrial environments.

### 2.2 Measurement-based techniques for robustness

In addition to the characterisation and planning, more recent research investigates the robust industrial wireless communications at the network usage stage, during which the deployed network is in use by clients. Extensive measurements are performed to enable a better insight into the robustness performance of various countermeasures against the harshness of industrial environments.

Through live tests in a mineral processing factory, the proposed lightweight packet error discriminator (LPED) was demonstrated to enable quick recovery from link outage [12]. Forward error correction is used in [13] to determine the error pattern in corrupted packets. This contributes to shorter detection time and boosts the reliability. The measurements in a paper mill and a paper roll warehouse demonstrated that the LPED accelerates link diagnostics by at least 190%, compared with the state-of-the-art (SOTA) approaches.

The bit- and symbol-error properties of industrial wireless sensor network were extracted and scrutinised in harsh industrial environments [14]. The measurement campaign was conducted at two paper mills and a paper warehouse during 14 days. The diversity of environments (highly reflective and absorbent) and setups (large and small separations, moving and static clutters, interfered and non-interfered links) provide a high degree of

generality to the measurements. Symbol interleaving was proven to outperform its bit counterpart.

In [15], the proposed methods predict radio signal coverage by considering typical industrial environments characterised by highly dense building blockage. They are corroborated by measurements in an oil refinery site.

Although these investigations perform extensive measurements, they have an assumption that the wireless connections are well maintained. There is very limited literature focusing on the case where a wireless link may become disconnected due to shadow fading on the shop floor.

### 2.3 Wireless standards for industry

Although IEEE 802.11/WiFi is a dominant technology with a common familiarity, it is currently deemed unsuitable for industrial applications, e.g. real-time control and localisation. Various researches are dedicated to the enhancement of industrial WiFi performance. A QoS-enabled 802.11 network is presented in [16], which considers real-time constraints for connecting industrial intelligent devices and controllers. In [17], redundant wireless adapters share information about the outcome of acknowledged transmissions, in order to have an enhanced media access control (MAC) for reliable WiFi networks. In [18], two alternative rate adaptation techniques for IEEE 802.11 are designed to meet the specific requirements of industrial communication systems. However, they all focus on modifying WiFi standards, where commercial off-the-shelf (COTS) devices cannot be used anymore.

Other wireless technologies also have limitations in satisfying the critical industrial requirements. Specifically, WirelessHART is an emerging wireless technology dedicated to industrial systems due to its high reliability and robustness. Its MAC layer is based on globally synchronised multi-channel time division multiple access which performs channel hopping at each slot. Its network layer supports multi-path multi-hop routing to provide robust routing [19]. It is used by Jin *et al.* [20] to enable real-time mixed-criticality communication in wireless sensor-actuator networks. However, its high latency remains a challenge for real-time industrial control.

### 2.4 Scope of this paper

In this paper, the IEEE 802.11-compliant WLAN/WiFi is taken as a representative wireless technology to embody the proposed solution. The issue of interference is out of scope, but is included in the outlook. In a general sense, the robustness denotes a constantly high radio QoS which may combine one or more quantifiable metrics. Herein, the QoS is quantified as RSS. If the RSS values within a target environment all stay above a threshold, the whole environment is considered fully covered and the robustness is achieved. The countermeasures against the coverage hole focus on deploying COTS hardware by using the redundancy of the over-dimensioned and reconfigurable network.

### 3 Solution presentation

The proposed solution includes sequential components for industrial indoor robust wireless communications. Each component will be introduced in the following subsections. This solution is implemented as a unified system running on a computer, which serves as a central controller. A Zotac® ZBox mini-PC (personal computer) is deployed in Linux Ubuntu. It uses the wavemon command line tool to gather RSS indicator (RSSI) from a target access point (AP). The mini-PC is attached to the top of a mobile robot. The measurement of mini-PC and the mobility of robot are both controlled by the central controller. Besides, the central controller encompasses the SUMO Matlab® toolbox [21] to optimise the measurement path and to visualise the data, and WHIPP (a heuristic indoor wireless propagation prediction tool [22]) for proof-of-concept simulation.

#### 3.1 Calibration

The RSSI is a good indicator of radio channel performance since it is vendor independent. However, there exists a discrepancy between the RSSI and the radio frequency (RF) power in practice. The mapping is not standardised. It is done by each wireless chipset manufacturer separately and is locked to the public, which may therefore be subject to inaccuracies. Furthermore, COTS wireless products based on these chipsets contain additional circuitry, printed circuit board lanes, and soldered connectors around the chipset, which causes an additional deviation between the two parameters.

To this end, two types of measurements are designed to be performed simultaneously: (i) RSSI measurements by a client mobile PC equipped with COTS antennas, and (ii) the actual RF power measurements by a spectrum analyser. As the frequency 2.4 GHz is often used, the corresponding lambda (i.e. the wavelength) is 12.5 cm. The two transmitting and two receiving antennas are mounted about 10 cm apart from each other, which means large-scale fading is eliminated as a source of deviation between the RSSI and RF power (10 cm is much shorter than 10 lambda) while the antennas do not obstruct each other's reception (10 cm is farther than lambda/2). Additionally, the same antennas and antenna feeder cables are used for both measurements. Therefore, solely the different transmit power for both types of measurements influence the difference between the measured RSSI and RF power.

#### 3.2 Automatic measurements

Once the measurement setup is calibrated, measurement campaigns are automatically carried out through the central controller. The mobility of measurements can be enabled by integration of measurement setups onto various industrial movable infrastructures, e.g. AGVs, mobile robots, cranes, forklifts, and so on. The measured RSSI data are tagged with 2D physical locations. Specifically, for robot mobility control, a hybrid sequential design algorithm is proposed within the SUMO Matlab® toolbox, installed in the central controller.

This algorithm starts from the initial design, where a small set of measurements are chosen in a space-filling manner. Then it sequentially specifies additional measurements to be performed at optimal locations until the overall pattern is characterised, named sequential design. In both designs, a minimal number of maximally informative measurements are given by this algorithm, while all variations in RSSI values are characterised, and the total distance travelled by the robot is minimised.

**3.2.1 Initial design:** In literature, several algorithms are available to generate a suitable set of initial data samples, e.g. Latin hypercube design, random sampling, orthogonal arrays, uniform grid, and so on. Such designs are well studied in the case of point-based measurements. For the automatic mobile measurement path, it is preferable to measure along a Hilbert curve that specifies a sequence of trajectories having space-filling properties. A Hilbert

curve is basically a Lindenmayer system that can be expressed using the following production rules for axiom 'X'

$$\begin{aligned} X &\rightarrow -YF + XFX + FY- \\ Y &\rightarrow +XF - YFY - FX+ \end{aligned} \quad (1)$$

where the symbols  $F$ ,  $+$ , and  $-$  are constant implying moving forward, turning right by  $90^\circ$ , and turning left by  $90^\circ$ , respectively.

**3.2.2 Sequential design:** In the general sense, the order of the Hilbert curve remains to be decided for each application case. If it is chosen too low, the initial set of measurements might be too sparse in certain regions. Therefore, additional measurements must be performed. The spatial location of these additional measurements is determined by using the LOLA-Voronoi algorithm [23], which balances exploration of the whole environment and exploitation of interesting regions.

The exploration component is based on a Voronoi tessellation that divides the measurement field into disjoint cells. Each cell comprises the points that are closer to one particular measured sample as opposed to any other measured samples. The sparser regions in the field will therefore be covered by larger Voronoi cells, in which additional samples are preferably chosen. The exploitation component focuses on regions where the corresponding RSSI values show rapid variations. Such regions usually need more measured data to be characterised and modelled accurately. To this end, measurements should be performed in regions where the estimated non-linearity of those values is the highest, based on neighbourhood selection and local linear approximations. Both components are combined into a metric that balances both of them and guides the sample selection.

#### 3.3 Over-dimensioning

On the basis of the former automatic measurements, a novel approach, named 'over-dimensioning', is designed for AP planning and deployment. It guarantees that each target location on a shop floor is able to be covered by at least two APs. It includes the following steps.

**3.3.1 PL model establishment:** The data collected from automatic measurements can be used to characterise the radio propagation in indoor factories. By considering exclusively the large-scale fading, PL (in dB) is calculated as

$$PL = P_{Tx} + G_{Tx} + G_{Rx} - \langle P \rangle \quad (2)$$

where  $P_{Tx}$  is the transmit power,  $G_{Tx}$  and  $G_{Rx}$  are the Tx and Rx antenna gains, and  $\langle P \rangle$  is the RF power samples (in dBm) which are averaged over a distance of several lambdas (to eliminate the small-scale fading, while having approximately the same PL).

Furthermore, PL samples can be fitted in the following form

$$PL(d) = PL0 + 10n \cdot \log_{10}(d) + \xi \quad (3)$$

where  $PL0$  is the PL at the reference distance of 1 m (in dB),  $n$  is the PL exponent which is a dimensionless parameter indicating the increase in PL with distance, and  $\xi$  is the deviation between measurement and model (in dB).

**3.3.2 Demand estimation:** A clear view should be gained on the maximum throughput demand of the target industrial region, in order to accordingly determine the capacity of each AP. As a result, it is necessary to identify and forecast the wireless application per client, per time unit, and per room in the target factory. Each application has its corresponding bit rate range. Table 1 presents some common industrial wireless applications and their reference bit rates. The required throughputs can be further converted into the corresponding sensitivity according to existing literature. An illustrative mapping for 802.11 g at 2.4 GHz is indicated in Table 1. Whether this required throughput is

actually achieved depends not only on the received power, but also on the number of simultaneous users, the interference, protocols on higher layers, and so on. Nevertheless, this is out of scope of this paper, and can be explored in future work.

**3.3.3 Over-dimensioning:** Fig. 1 gives an illustration of the over-dimensioning philosophy. Herein one shop floor is by default considered to be so large that at least two APs need to be deployed for a full or quasi-full coverage. A redundant coverage is brought by over-dimensioning. This is similar to the philosophy of mesh networks, where redundant paths exist for robustness. However, the distinction is that the over-dimensioning is rather a physical approach, while the mesh is on the network layer. A redundant coverage is essential for robust industrial wireless communications, where the radio propagation easily becomes susceptible to the dynamic disturbance, e.g. moving objects and human operators which cause short-term shadowing, and reorganised production lines which cause long-term shadowing. As a consequence, an obvious QoS degradation may occur randomly and frequently. In case that the QoS provided by a link is or is predicted to be threatened, the network will start the reconfiguration to maintain a good QoS (see Section 3.4.2). Therefore, over-dimensioning serves as a network design strategy for robustness by increasing AP/link redundancy against temporal changes in AP/link states or properties. Instead of requiring a long-term change to the communication protocol stacks, COTS hardware can still be used.

### 3.4 Reconfiguration

When the deployed network is in use, automatic measurements increase the network's diagnostic capability, and the network reconfigurability aims at dealing with shadowing problems which occur quite randomly on the target shop floor.

**3.4.1 Measurement-based monitoring:** The distributed mobile measurement setups automatically conduct measurements around the shop floor and return real-time feedback. The sequential design (see Section 3.2.2) can be applied to enhance the measurement efficiency – only a limited number of locations are automatically selected for additional measurements. Furthermore, the fixed APs and wireless clients can monitor the radio environment themselves, and thus provide additional feedback to

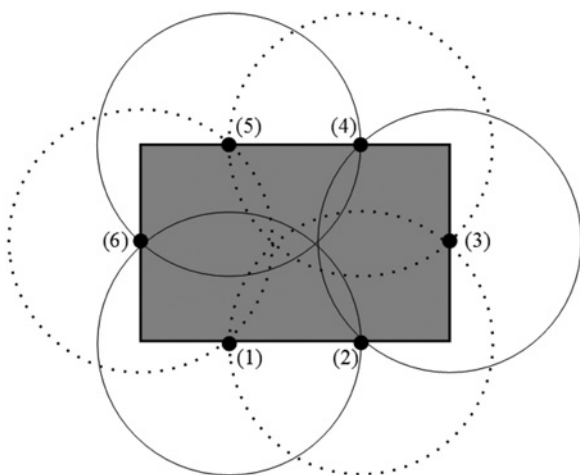


**Fig. 1** Proof-of-concept demonstration for over-dimensioning: each location on the shop floor is conceptually covered by at least two APs. The light orange rectangle denotes a general shop floor. The small solid circles represent APs. The APs are placed on the bounds of the shop floor according to the order indicated by the numeric beside each AP. Situated in the centre, each AP has a large hollow circle around it, standing for this AP's coverage. The group of solid and dotted circles corresponds to an individual and complete set of APs that can cover the whole shop floor, respectively

the central controller. Consequently, the real-time feedback effectively provides information on the radio environment to the central controller.

On the basis of measured QoS values, a surrogate model can be constructed by using the Kriging interpolation algorithm in the SUMO toolbox. This model contributes to a REM, which presents the spatial distribution of QoS values over the target environment. Triggered by predefined events, the central controller updates the REM. The trigger events can be various, e.g. receiving a predefined amount of latest feedback measurements, a certain time period, a change of industrial indoor topography, the model uncertainty surpassing an interpolation error threshold, and so on. Therefore, the latest surrogate model characterises the current environment, and facilitates the network reconfiguration for staying robust.

**3.4.2 Network reconfiguration:** Once a weak region is indicated by the REM and stays unimproved during a defined judging period, a proper network reconfiguration will be cognitively triggered to achieve the 'best coverage'. The network reconfiguration can be illustrated as powering on/off APs, switching power levels of APs, switching radio channels, and so on. The judging period, trigger events, and criteria for finding the 'best coverage' can all be varied, and depend on a specific industrial case. For instance, the defined period can be 2% of the scheduled production period for a certain production line. During this defined period, the indicated region is continuously focused on and evaluated with the REM. A trigger event can be that <95% of the whole shop floor is wirelessly covered. The 'best coverage' can be the largest coverage on the shop floor, an always-guaranteed coverage on some emphasised regions where there is a prioritised requirement for continuous throughput provision, and so on.

## 4 Empirical studies

The measurement parts of the proposed solution were demonstrated in real industrial environments. The involved truck factory is located at Flanders, Belgium, including a truck factory and an AGV factory.

### 4.1 Calibration

The mapping between the RSSI and the true RF power was quantified based on measurements in the production hall of the truck factory. Fig. 2 shows the mobile robot based measurement setup involved in this calibration. At the Tx side, which is fixed, a D-Link DI-624+ AP sends wireless packets on WiFi channel 1 with a transmit power of 7 dBm. For the received RF power measurements, a signal generator transmits a continuous wave signal at 2470 MHz with a power of 14 dBm. This frequency is sufficiently separated from the frequency band used by channel 1, to avoid interference with the RSSI measurements.

At the mobile Rx side, the whole measurement equipment is mounted on the robot's platform, shown by Fig. 2b. The Zota<sup>®</sup> ZBox mini-PC collects RSSI in channel 1 on the IEEE 802.11b/g standard interface. A Rohde & Schwarz FSL6 spectrum analyser is used to sample the true received RF power.

The robot randomly drives around, while the mini-PC and laptop continuously measure and store the RSSI and received RF power, respectively. The gathered RSSI and RF power samples are subsequently averaged to remove the small-scale fading caused by the slight displacement between Tx and Rx. The averaging interval is 10 wavelengths at 2470 MHz. The number of averaged RSSI samples equals 207 for the truck factory. Then, the transmit power is subtracted from the averaged RSSI and RF power samples, so both types of measurements appear to have the same transmit power of 0 dBm.

Fig. 3 shows the averaged and linearly shifted RSSI and RF power ( $\langle \text{RSSI} \rangle_{0 \text{ dBm}}$  and  $\langle P \rangle_{0 \text{ dBm}}$ , respectively) versus distance for the truck factory. It is clear that RSSI underestimates the true received RF power. The underestimation of the RSSI is then calculated as the

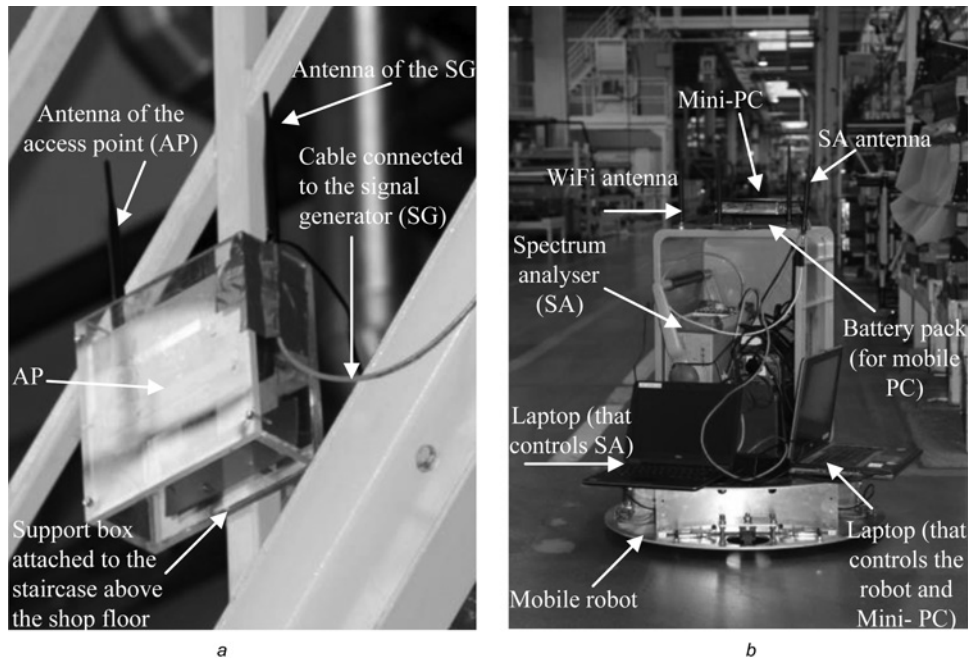


**Fig. 2** Mobile robot measurement setup and industrial environment example

a Transmitter (Tx) side  
b Receiver (Rx) side

difference  $\langle P \rangle_{\text{dBm}} - \langle \text{RSSI} \rangle_{\text{dBm}}$  between corresponding values at the same Tx–Rx distance. A conservative assessment of the RSSI underestimation (denoted as  $M$ ) is then determined as the fifth percentile of these differences. During the network planning stage,  $M$  is added to the measured RSSI samples to estimate the true received RF power, and is conservative in the sense that it does not overestimate the RF power. For the Zotac<sup>®</sup> ZBox mini-PC,  $M$  was found to be equal to 9.46 dB. It stays the same as long as the pair of ‘AP + client + antennas’ is unchanged. The clear awareness of the discrepancy between RSSI and RF power enhances the precision of the entire system, since the system works on sensitivity (i.e. RF power) instead of RSSI (see Table 1, Sections 3.3 and 5).

#### 4.2 Automatic measurements

The RSSI measurements for the network planning were conducted in the AGV factory, with the same setup as the one in Fig. 2b, except

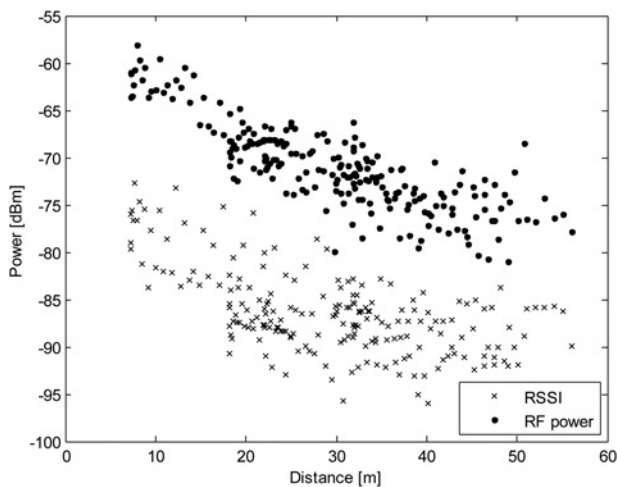


**Fig. 3** Averaged and shifted RSSI and received RF power versus distance for the truck factory. RSSI was found to underestimate the received RF power. A linear shift was further found to be 9.46 dB in the fifth percentile

that the spectrum analyser, together with the connected laptop, was not used any longer. The integration of measurement setups with a mobile robot was carried out. The measured data is in JSON format. The measurement setups store the measured data on their local CouchDB databases, which synchronise with the central controller using the measured WiFi network.

On the basis of 719 RSSI samples by using the initial design and sequential design (see Section 3.2), a Kriging surrogate model was built and validated on a separate set of 268 measurements that were performed at random locations within the area covered by the second-order Hilbert curve (see Fig. 4). This surrogate model contributes to a REM (see Fig. 4). For the purpose of a reliable evaluation on the quality of the obtained surrogate model, a root-relative-square error (RRSE) was applied to the model within this measurement validation set as follows

$$\text{RRSE}(\mathbf{y}, \tilde{\mathbf{y}}) = \sqrt{\frac{\sum_{i=1}^n (y_i - \tilde{y}_i)^2}{\sum_{i=1}^n (y_i - \bar{y})^2}} \quad (4)$$

where the two vectors  $\mathbf{y}$  and  $\tilde{\mathbf{y}}$ , respectively, contain the true and predicted RSSI values, and the scalar  $\bar{y}$  is the mean true RSSI value, respectively. It was found that the resulting Kriging model achieved a RRSE of 0.2945, which is fairly low, since a RRSE has a range from 0 to the positive infinity. What is more, the Pearson correlation coefficient of the two vectors  $\mathbf{y}$  and  $\tilde{\mathbf{y}}$  was also calculated. It can lie between  $-1$  (total negative correlation) and  $1$  (total positive correlation), and is defined as

$$\rho_{\mathbf{y}, \tilde{\mathbf{y}}} = \frac{\text{cov}(\mathbf{y}, \tilde{\mathbf{y}})}{\sigma_{\mathbf{y}} \sigma_{\tilde{\mathbf{y}}}} \quad (5)$$

where  $\text{cov}$  is the covariance, and  $\sigma_{\mathbf{y}}$  and  $\sigma_{\tilde{\mathbf{y}}}$  are the standard deviations of  $\mathbf{y}$  and  $\tilde{\mathbf{y}}$ , respectively. In this investigation, it was 0.9625. This implies a strong correlation between the actual RSSI behaviour and that predicted by the model.

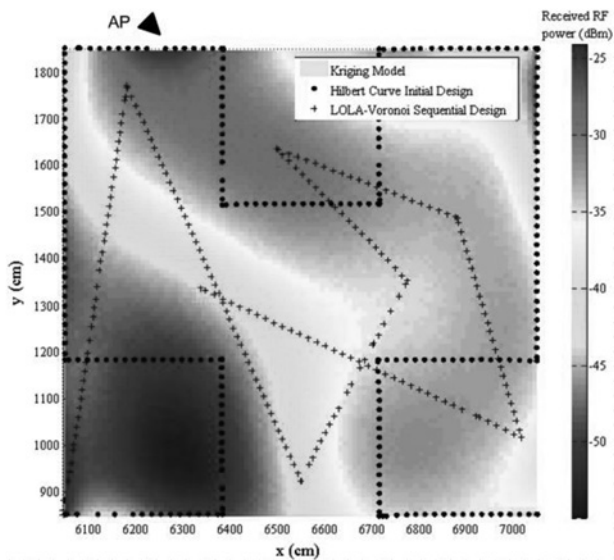


**Fig. 4** REM, shown on the central controller, specifically indicating RSSI spatial distribution. The AP is placed about 3 m outside the top-left region of the REM, and is oriented towards the neighbourhood of the point (7000, 1400). The mobile robot automatically performs measurements, by following the second-order Hilbert curve (dots) first, and then the LOLA-Voronoi sequential design (crosses). The Hilbert curve measurement path design tries to cover the test environment as evenly as possible, whereas the LOLA-Voronoi algorithm focuses on complementary measurements in locations where the RSSI values are highly dynamic

## 5 Proof-of-concept simulation

In this section, simulation is performed in WHIPP. All types of AP configurations and physical building layouts are able to be handled in WHIPP. An empirical propagation model is first established statistically, based on the previously calibration and measured RSSI. A brief scenario is then created to demonstrate the concept of reconfiguration of the over-dimensioned network for robust industrial indoor radio communications.

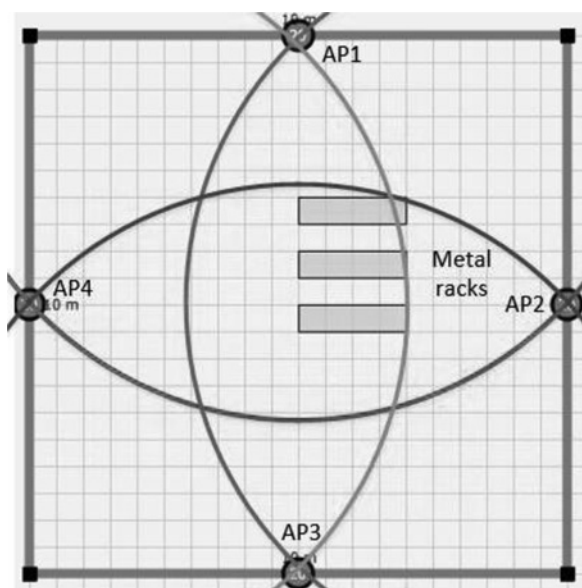


**Fig. 5** Simulation of over-dimensioning in the WHIPP tool. Each arc represents the coverage range of an AP. Each location in the factory hall is covered by at least two APs

### 5.1 Empirical propagation model

The unknown parameters in (3) are determined through multiple regression.  $PL_0$  is equal to 46.91, and  $n$  is 1.96. The error term  $\xi$  is assumed to follow a zero-mean Gaussian distribution with standard deviation  $\sigma$  (in dB), which equals 2.39 dB. The model's coefficient of determination  $R^2$  amounts to 0.73, which shows that an appreciable amount of PL variability is explained by the  $\log_{10}(d)$ -dependency.

Besides, the attenuation loss caused by metal storage racks in another hall was measured by placing two Rx: one Rx was in line-of-sight (LOS) with the Tx, and the other Rx was in non-line-of-sight (NLOS) with a metal rack between the Tx and Rx. The average received power along the LOS track is equal to  $-49.5$  dBm, while the average received power along the NLOS track is  $-54.1$  dBm. The metal rack attenuation loss is thus the difference between both values, i.e. 4.6 dB.

### 5.2 Over-dimensioning

The over-dimensioning algorithm was implemented in WHIPP. The following configurations are considered. (i) The simulated environment is a factory hall that has the same size as that in Fig. 4 ( $10\text{ m} \times 10\text{ m}$ ), and is composed of concrete walls. (ii) There is no AP previously installed within the hall. APs can only be placed on the walls, using IEEE 802.11g. (iii) The first AP is placed in the middle of the wall. (iv) The previously obtained PL model is used and three metal racks are present.

Fig. 5 presents the four APs planned and deployed by over-dimensioning in the simulation environment. It is obvious that each AP is placed in the middle of a hall wall, with two adjacent APs located on its coverage edge. Consequently, the four hall corners are covered by two APs, the centre area by four APs, and the remaining parts by three APs (see Fig. 5). This shows a strong coverage redundancy over the entire factory hall.

### 5.3 Network reconfiguration

To deal with the coverage gaps caused by shadow fading, the over-dimensioned APs are intelligently controlled in WHIPP for simulation. The empirical model obtained in Section 5.1 is used.

**5.3.1 Smart AP switch mechanism:** For an illustration of network reconfiguration, a smart AP powering on/off mechanism is used to validate the conceptual capacity for keeping robust against the dynamics in an industrial indoor environment. Once the four APs are over-dimensioned, only one is switched on, while the other three are switched off during the normal usage course. Standby mode is out of consideration since switching off contributes to a maximal energy saving. Alternative strategies are possible. For instance, the APs could stay on, but not operational, ensuring better responsiveness at the cost of higher energy consumption. The smart switch mechanism was further simulated in WHIPP. The initial scenario is that some metal racks cause shadowing effects on the region behind them. The minimum required received power ( $P_{RxMin}$ ) for each location was set as  $-68$  dBm (which is the highest reference RF power for 802.11g), considering that each location has the same throughput requirement as the remote video monitoring. A location point is considered as covered if its receiving radio power is greater than  $P_{RxMin}$ . An area's coverage rate ( $R_c$ ) is the ratio of the number of covered location points within this area to the area's total number of location points. The target for the smart switch to search for the best solution (or for the network to stay robust against shadow fading) is that  $R_c$  should not be  $<95\%$ . The previous empirical model was used in the link budget calculation.

**5.3.2 Simulation:** As illustrated in Fig. 6a, the metal racks obviously impede the radio propagation from AP1 to the bottom right region. As a consequence, its  $R_c$  drastically drops to 46% (see Table 2), i.e. less than half of the hall is covered.

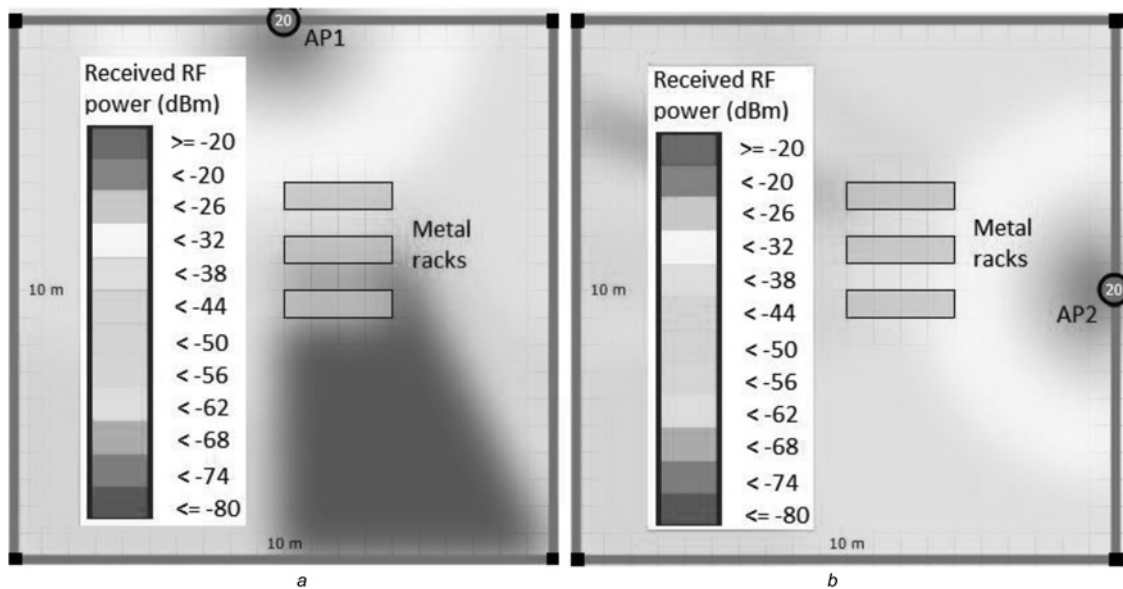


**Fig. 6** Current AP on/off state and the optimal solution proposed by smart switch in the simulation case. The APs, which are over-dimensioned (see Fig. 5) but are switched off, are not shown on the two maps

a Current AP on/off state  
b Smart switch

**Table 2** Example for cognitive decision making of the smart switch

Solution	AP1	AP2	AP3	AP4	Coverage rate $R_c$ of the target region, %	Mean received RF power, dBm
1	on	off	off	off	46	-59
2	off	on	off	off	100	-36
3	off	off	on	off	100	-40
4	off	off	off	on	100	-48

Conceptually, this weak coverage is sensed by mobile measurements, indicated by the REM (see Fig. 4), and stays poor during the defined judging period. Upon surpassing this judging period, the smart switch algorithm starts to search for the best solution to enhance the current coverage. As indicated in Table 2, the best solution, where only AP2 is switched on, achieves a  $R_c$  of 100% and the highest mean received RF power (-36 dBm). It is further visualised in Fig. 6b. Consequently, the 'always-on' availability of the WLAN is ensured in the hall, and the robustness is guaranteed.

## 6 Conclusions

In this paper, a measurement-based solution is proposed for robust radio communications in harsh industrial environments. It harmoniously integrates a range of SOTA and novel wireless approaches with a focus on large-scale fading. The approaches include calibration, automatic measurements, over-dimensioning, and network reconfiguration. This solution took IEEE802.11/WiFi as a representative wireless technology for case studies. It was jointly demonstrated in two real factories and in the radio simulation tool WHIPP.

For the calibration, two measurements were conducted simultaneously: (i) RSSI measurements by a client mini-PC which is equipped with COTS antennas, and (ii) the real RF power measurements by a spectrum analyser. An evident difference of 9.46 dB was found between the RSSI and real RF power. This reveals the importance of calibration when using a new pair of 'AP + client + antennas' for RSS measurements.

For mobile measurements, the measurement setups were integrated with an AGV and a mobile robot. The mobility of the

robot was further controlled by the surrogate modelling technique for optimal measurements and for building the REM. Through a minimised number of measurements, the REM was built. The RRSE was 0.2945 and Pearson correlation was 0.9625, which indicates a reliable interpolation precision for wireless monitoring.

In the simulation which was based on the measured data, APs were over-dimensioned such that each location in the target environment was covered by at least two APs. Metal racks were moved into the environment which was originally empty. Severe shadowing was observed in the simulation. As a method of network reconfiguration, the smart AP switch mechanism made use of the redundant APs to ensure a full network availability by recovering the observed coverage hole. A 100% coverage was finally observed after the network reconfiguration.

As an extension work, measurements can be conducted by placing between Rx-Tx multiple metal racks which block the LOS microwave propagation. Besides, more radio QoS metrics may be jointly considered to quantify the robustness, in addition to RSS. For instance, jitter and latency are crucial for the automation control, where a real-time traffic is generally produced. With the proposed mobile measurement setups, it is easy and economical to collect these QoS metrics from the perspective of clients.

Besides the harshness of industrial environments, several radio sources may coexist in factories, e.g. WiFi, Bluetooth, ZigBee, and microwave oven. The occupied frequency channels may be overlapped. Therefore, interference is another issue that challenges the robustness of industrial radio communications. It is envisioned to be taken into consideration in future work. The potential means to cancel or minimise interference include intelligent channel switch, diversity (time, frequency, and space) schemes, effective radio resource management, and so on.

## 7 Acknowledgment

Emmeric Tanghe and Dirk Deschrijver are post-doctoral researchers of FWO-Vlaanderen. This research was supported by the FORWARD project (<https://www.iminds.be/en/projects/2014/03/20/forward>). The FORWARD project is co-funded by iMinds (Interdisciplinary Institute for Technology), a research institute founded by the Flemish Government.

## 8 References

- 1 Drath, R., Horch, A.: 'Industrie 4.0: hit or hype?', *IEEE Ind. Electron. Mag.*, 2014, **8**, (2), pp. 56–58
- 2 Evans, P.C., Annunziata, M.: 'Industrial internet: pushing the boundaries of minds and machines'. General Electric white paper, 2012
- 3 Radziwon, A., Bilberg, A., Bogers, M., *et al.*: 'The smart factory: exploring adaptive and flexible manufacturing solutions', *Procedia Eng.*, 2014, **69**, pp. 1184–1190
- 4 Cisco and Rockwell automation white paper: 'Wireless design considerations for industrial applications: design and deployment guide', March 2014, pp. 5–6
- 5 Plets, D., Joseph, W., Vanhecke, K., *et al.*: 'Exposure optimization in indoor wireless networks by heuristic network planning', *Prog. Electromagn. Res.*, 2013, **139**, pp. 445–478
- 6 Akerberg, J., Gidlund, M., Lennvall, T., *et al.*: 'Chapter 4: design challenges and objectives in industrial wireless sensor networks', in Hancke, G.P. (Ed.): 'Industrial wireless sensor networks – applications, protocols and standards' (CRC Press, 2013)
- 7 Chrysikos, T., Papadacos, C., Kotsopoulos, S.: 'Wireless channel measurements and modeling for an office topology at 3.5 GHz'. Wireless Telecommunications Symp., New York, USA, April 2015, pp. 1–6
- 8 Zhu, J., Wang, H., Hong, W.: 'Characterization of large-scale fading for 45 GHz indoor channels'. third Asia-Pacific Conf. on Antennas and Propagation, Harbin, China, July 2014, pp. 728–730
- 9 Kremono, H., Nakagawa, K., Altintas, O., *et al.*: 'Characterization of first and second order statistics of large scale fading using vehicular sensors'. IEEE 81st Vehicular Technology Conf., Glasgow, Scotland, May 2015, pp. 1–5
- 10 Tanghe, E., Joseph, W., Verloock, L., *et al.*: 'The industrial indoor channel: large-scale and temporal fading at 900, 2400, and 5200 MHz', *IEEE Trans. Wirel. Commun.*, 2008, **7**, (7), pp. 2740–2751
- 11 Liu, N., Plets, D., Goudos, S.K., *et al.*: 'Multi-objective network planning optimization algorithm: human exposure, power consumption, cost, and capacity', *Wirel. Netw.*, 2015, **21**, (3), pp. 841–857
- 12 Barac, F., Caiola, S., Gidlund, M., *et al.*: 'Channel diagnostics for wireless sensor networks in harsh industrial environments', *IEEE Sens. J.*, 2014, **14**, (11), pp. 3983–3995
- 13 Barac, F., Gidlund, M., Tingting, Z.: 'LPED: channel diagnostics in WSN through channel coding and symbol error statistics'. IEEE Ninth Int. Conf. on Intelligent Sensors, Sensor Networks and Information Processing, Singapore, April 2014, pp. 1–6
- 14 Barac, F., Gidlund, M., Zhang, T.: 'Scrutinizing bit- and symbol-errors of IEEE 802.15.4 communication in industrial environments', *IEEE Trans. Instrum. Meas.*, 2014, **63**, (7), pp. 1783–1794
- 15 Savazzi, S., Rampa, V., Spagnolini, U.: 'Wireless cloud networks for the factory of things: connectivity modeling and layout design', *IEEE Internet Things J.*, 2014, **1**, (2), pp. 180–195
- 16 Cena, G., Seno, L., Valenzano, A.: 'On the performance of IEEE 802.11e wireless infrastructures for soft-real-time industrial applications', *IEEE Trans. Ind. Inf.*, 2010, **6**, (3), pp. 425–437
- 17 Cena, G., Scanzio, S., Valenzano, A., *et al.*: 'An enhanced MAC to increase reliability in redundant Wi-Fi networks'. IEEE 10th Workshop on Factory Communication Systems, Toulouse France, May 2014, pp. 1–10
- 18 Vitturi, S., Seno, L., Tramarin, F., *et al.*: 'On the rate adaptation techniques of IEEE 802.11 networks for industrial applications', *IEEE Trans. Ind. Inf.*, 2013, **9**, (1), pp. 198–208
- 19 Haibo, Z., Soldati, P., Johansson, M.: 'Performance bounds and latency-optimal scheduling for converge cast in WirelessHART networks', *IEEE Trans. Wirel. Commun.*, 2014, **12**, (6), pp. 2688–2696
- 20 Jin, X., Wang, J., Zeng, P.: 'End-to-end delay analysis for mixed-criticality WirelessHART networks', *IEEE/CAA J. Autom. Sin.*, 2015, **2**, (3), pp. 282–289
- 21 Gorissen, D., Couckuyt, I., Demeester, P., *et al.*: 'A surrogate modelling and adaptive sampling toolbox for computer based design', *J. Mach. Learn. Res.*, 2010, **11**, pp. 2051–2055
- 22 Plets, D., Joseph, W., Vanhecke, K., *et al.*: 'Simple indoor path loss prediction algorithm and validation in living lab setting', *Wirel. Pers. Commun.*, 2013, **68**, (3), pp. 535–552
- 23 Crombecq, K., Gorissen, D., Deschrijver, D., *et al.*: 'A novel hybrid sequential design strategy for global surrogate modeling of computer experiments', *SIAM J. Sci. Comput.*, 2011, **33**, (4), pp. 1948–1974